

TRAPPED WAVE ANTENNAS

Herman Ehrenspeck, Werner Gerbes and Francis J. Zucker

Air Force Cambridge Research Center
Cambridge, Mass.

SUMMARY

The question is first raised as to how a 'trapped' wave radiates, and what beam shapes it can produce. The results are compared with the radiation fields produced by conventional antenna apertures.

A flush-mounted type of antenna is discussed which utilizes waves trapped in single and multiple dielectric layers. The calculated mode characteristics are in very good agreement with experimental results. By means of phase and amplitude control, it should be possible to design such antennas with a great variety of beam shapes in azimuth and elevation.

HOW DOES A TRAPPED WAVE RADIATE?

A surface wave is one which propagates along an interface between two media. If the surface wave is slower than light, it carries most of its energy within a small distance from the interface, and will not radiate unless a discontinuity impedes its progress. We can therefore speak of it as a guided, or 'trapped' wave. Its phase fronts are perpendicular to the interface (see Fig. 1), while the amplitude decays exponentially upward.

The general theory of surface waves has been described elsewhere.¹ Here we are concerned with the manner in which a surface wave radiates, and with the types of pattern it can produce. We will also discuss phase control on dielectric sheets, as a prerequisite for beam shaping in practice.

At first sight the expression 'trapped wave antennas' appears like a contradiction in terms. How can a wave be 'trapped' and radiate at the same time? To explain this, we consider an infinitely long unshielded waveguide (dielectric slab or corrugated surface.) One or more trapped modes will propagate along it. They do not radiate as long as the guide is uniform. If the guide is cut short, however, to form a finite slab, then a radiation pattern is set up. This means that the existence of an electromagnetic far-field is somehow connected with the missing parts of the infinite surface. As usual, the far-field pattern is obtained by integrating over the tangential E or H field along the slab surface. Choosing the origin of coordinates in the center of the slab, and paying attention only to the limits of integration, we note first that

$$\int_{-\infty}^{\infty} = 0$$

(no radiation). This implies, however, that

$$\cdot \int_{-\infty}^{-d/2} + \int_{-d/2}^{d/2} + \int_{d/2}^{\infty} = 0, \text{ or } \int_{-d/2}^{d/2} = - \int_{-d/2}^{-d/2} - \int_{d/2}^{\infty}$$

In words: the radiation pattern of the finite slab is equal in magnitude and opposite in phase to the pattern of the two semi-infinite slabs which have been cut away.

We can shuffle the limits of integration in another way, more useful than the first:

$$\int_{-d/2}^{d/2} = \int_{-\infty}^{d/2} - \int_{-\infty}^{-d/2}$$

(see Fig. 2). This shows that the finite-panel pattern can be regarded as a superposition of the patterns of two semi-infinite panels, with origin at $-d/2$ and $d/2$, respectively. The two panels are fed out of phase by the time it takes the trapped wave to travel from $-d/2$ to $d/2$, plus a delay of π' occasioned by the phase-reversal of the shorter semi-infinite slab (minus sign in front of the last integral). To obtain maximum radiation in the end-fire direction, this phase delay must be compensated for by choosing d appropriately. We are merely restating here in physical terms the well-known Hansen - Woodyard condition, for which a number of pseudo-explanations have appeared in the literature from time to time.

It also appears from Fig. 2 that the far-field pattern of the longer semi-infinite slab could be obtained alternatively by integrating over a vertical plane through $d/2$ (vertical plane through $-d/2$ for the shorter semi-infinite slab). In this plane, the phase is constant and the amplitude decreases exponentially away from the slab (it is trigonometric within the slab). The radiation of the finite slab is therefore due to its two transverse planes of discontinuity. As before, the radiation from the plane through $d/2$ is delayed by the slow-travelling surface wave. In addition, we have the phase reversal for the aperture distribution in the plane through $-d/2$, because, just as before, we are supposed to subtract the $(-d/2)$ -pattern from the $(d/2)$ -pattern. Physically speaking, we might say that the phase reversal is due to the different nature of the field discontinuities at $-d/2$ and at $d/2$: in the first aperture the trapped wave is being set up, while in the second it is being terminated. At any rate, it is the front and the back end of the trapped wave which radiates, and there is no continuous leakage of energy along the slab surface itself.

We cannot go much further in our physical interpretation of the manner in which a trapped wave radiates. There seems to be little point in drawing lines of power flow from the finite slab to its far-field, since the impossibility of localizing energy in a Maxwellian field leads to an infinite number of power flow pictures, all equally correct.

WHAT BEAM SHAPES ARE OBTAINABLE FROM TRAPPED WAVE ANTENNAS?

Dunbar has shown² how to utilize travelling wave antennas for beam shaping. By suitable amplitude and phase control, it is possible to obtain shaped beams (such as csc^2) as well as patterns with deep nulls. Dunbar's design equations, as he himself noted, break down when the phase velocity of the travelling wave is less than that of light. This means that our trapped wave antennas are excluded from Dunbar's analysis. The question therefore arises as to the beam shapes obtainable from trapped wave antennas, and as to the variety of these beam shapes when compared to the faster-than-light travelling wave antennas.

Integration³ over the semi-infinite slab of Fig. 3 reveals that the radiation pattern due to a trapped wave is elliptic, with front-to-back ratio given by $(c + v)/(c - v)$. This assumes that the transition from slab to free space is made gradual enough to give rise to a negligible reflected wave. If an appreciable reflected wave does exist, its pattern will also be elliptic, but with reversed front-to-back ratio and a maximum amplitude equal to the incident wave amplitude multiplied by the reflection coefficient. In what follows, we shall omit this reflected wave pattern. Combining the two semi-infinite slab patterns according to the prescription in Section 1, we find by simple algebra that the finite slab pattern is of the conventional $\sin x/x$ form, with the added observation that the envelope of its polar plot is still the ellipse of the semi-infinite panel, doubled in amplitude but with the same front-to-back ratio.

Comparison with faster-than-light travelling waves shows (see Fig. 4) that the pattern of the semi-infinite antenna is now hyperbolic, with one branch of the hyperbola mirror-imaged about a vertical axis through the phase center. This results in a pattern infinity in the direction of the emerging main beam. The infinity disappears as soon as two hyperbolae are added (with suitable phase difference) to constitute a finite-aperture pattern. The conventional $\sin x/x$ polar plot emerges again, this time with hyperbolic envelope, and with maxima in the direction of the envelope infinities. The limiting case of $v = c$ results in a parabolic envelope, and applies to broadside arrays.

The stationary phase points which play an important part in Dunbar's analysis correspond to real angles of emergence for the main beam, and therefore do not appear in the far-field integral

for trapped waves. This suggests that a far greater variety of beam shapes is obtainable from fast-wave apertures than from trapped wave antennas. To achieve a prescribed radiation pattern it is necessary to vary the phase in the aperture so that the main beam emerges at a calculable real angle from each point on the antenna. This cannot be done for slow waves, since their angle of emergence is imaginary.

The situation is not quite as dark as it seems, for three reasons. To begin with, the pattern of a trapped wave antenna is always accompanied by the direct radiation of its feed. If the transition from waveguide to dielectric slab is sudden, as in Fig. 5, this feed radiation can be suppressed some 15 db or more below the energy transferred to the slab, and the total pattern is therefore essentially $\sin x/x$. If, on the other hand, a waveguide horn is used with gentle flare and large aperture to effect as gradual a transition to the open surface as possible, then the trapped wave appears to originate at minus infinity and the resulting pattern is elliptic. Putting it another way, the direct feed radiation is increased so as to fill in the deep nulls of the finite slab pattern, until in the limit the feed radiation exactly cancels the field due to the rear surface of discontinuity of the trapped wave, leaving us with the pattern of a semi-infinite slab. This shows that shaped patterns are in principle obtainable from trapped wave antennas.

The second reason is that the extent of the ground plane in which the trapped wave antenna is embedded can be utilized to influence the total pattern.⁴ Utilizing this method in conjunction with control over the direct feed radiation, Dr. M. Ehrlich⁵ succeeded in building a trapped wave antenna with excellent csc^2 pattern.

The third, and most important reason for optimism is based on the idea of phase and amplitude modulation along a trapped wave antenna. The first man to experiment with such an antenna was G.E. Mueller,⁶ although he did not analyze it from our present point of view. Fig. 6(a) illustrates his dielectric rod loaded with periodic disks of high dielectric constant. The disks bind their trapped wave so closely that its amplitude is negligible compared to the amplitude of the trapped wave on the rod itself; the disks are then spaced in such a way that the in-between sections of dielectric rod radiate in phase to yield a broadside pattern. Generalizing Mueller's idea, we may examine the far-field integral of any periodic phase and amplitude modulation, and soon discover the presence of one or more stationary phase points of the type utilized by Dunbar. In a recent conversation, Dr. J.C. Simon⁷ mentioned to one of us that he approached this problem via the Fourier spectrum of the modulated phase function which, when properly chosen, contains one or more lines corresponding to phase velocities faster than light. The decisive point is that Dunbar's beam shaping methods are now seen to be applicable to modulated trapped wave antennas, which therefore exhibit a wealth of pattern

potentialities equal to that of the fast-wave apertures and the unmodulated trapped wave antennas combined.

The antenna of Fig. 6(a) contains sharp discontinuities which cause reflections and high side lobes. To avoid these difficulties, the gentler modulation shown in Fig. 6(b) is proposed. This figure shows a dielectric slab above a metal sheet, first in longitudinal cross-section, and then from above. The periodicity in any given cross-section is so low that the resulting pattern would be multi-lobed. It will therefore be necessary to stagger the cross-sections in the manner shown and thus cancel the extraneous lobes. We hope to test such a "washboard" antenna in the near future.

PHASE CONTROL ON DIELECTRIC SHEETS

It is clear from the foregoing that success in beam shaping with trapped wave antennas rests on the possibilities of phase and amplitude control. This requires, first of all, a knowledge of the TE and TM modes in slabs and multiple layers. The modal properties are usually determined by solving a transverse eigenvalue problem, which can alternatively be expressed as a transverse resonance condition. We decided, however, to carry out the modal analysis by a new method, due to one of us (W. Gerbes). It introduces the Laplace transform to permit application to arbitrary pulse shapes propagating along the slab, and uses matrix notation to allow for an arbitrary number of layers. Only plane sheets have been considered thus far.

Figures 7 to 10 deal with the properties of the lowest TE and TM mode in a slab of thickness τ_2 spaced at a height τ_1 above a perfectly conducting ground plane. A given phase velocity can be realized in an infinite number of ways. If we start with a slab directly lying on metal, we can keep the phase velocity of a TM mode constant by raising the slab off the surface and increasing its thickness at the same time, until at very large distance from the ground plane it is twice what it was to begin with. To keep the phase velocity of a TE wave constant, the slab would have to lose in thickness as it is raised upward.

The dotted line in Figs. 7 and 8 gives those values of slab and air-gap thickness for which the phase velocity is the same in the TM and the TE mode. These are therefore the geometric configurations for which a dielectric trapped wave antenna can be elliptically polarized. If both modes are excited with equal strength, the resulting polarization is circular. Fig. 9 shows the conditions for elliptic polarization once more, and illustrates furthermore that the mode velocities are always restricted within a band terminated by the velocity of light on one side and by the free propagation velocity in an infinitely large dielectric slab on the other.

A large number of data were taken by one of us (H. Ehrenspeck) to verify the theoretical predictions of mode characteristics. The excellent agreement shown in the right half of Fig. 10 is typical of the results. The worst deviations obtained are those shown in the left half of the figure. They occur when the slab lies directly on the metal surface, and are due to the minute but non-negligible air gaps still between them. A simple error calculation was made, with the result that a good fit was obtained for an average air gap thickness as indicated on the figure.

When more than one slab is used, the number of different geometrical structures corresponding to a single phase velocity increases further. Fig. 11 shows three possible configurations (drawn to scale), all yielding the same phase velocity. The general formula for multiple layers is as follows:

$$\text{th}_1 = \frac{\frac{d}{r+1} - \sum_{\nu}^{\nu} \lambda_{\nu} \text{th}_{\nu} + \frac{d}{r+1} \sum_{\mu}^{\mu} \sum_{\nu}^{\nu} \frac{d_{\nu}}{d_{\mu}} \text{th}_{\mu} \text{th}_{\nu} -}{1 - \frac{d}{r+1} \sum_{\nu}^{\nu} \frac{1}{d_{\nu}} \text{th}_{\nu} + \sum_{\mu}^{\mu} \sum_{\nu}^{\nu} \frac{d_{\mu}}{d_{\nu}} \text{th}_{\mu} \text{th}_{\nu} -} - \frac{\frac{\phi}{\mu} \frac{\nu}{\nu} - \sum_{\mu}^{\mu} \sum_{\nu}^{\nu} \frac{d_{\nu} d_{\mu}}{d_{\mu} d_{\nu}} \text{th}_{\mu} \text{th}_{\nu} + \dots}{-\frac{d}{r+1} \sum_{\mu}^{\mu} \sum_{\nu}^{\nu} \frac{d_{\mu}}{d_{\mu} d_{\nu}} \text{th}_{\mu} \text{th}_{\nu} + \dots}$$

where

$$\phi > \mu > \nu > 1$$

and

$$\text{th}_{\nu} = \tanh ik_{\nu} \tau_{\nu}$$

(k is the transverse wave number),

$$d_{\mu} = \epsilon_{k\mu} / \epsilon_{fc} k_1,$$

and where the layers are numbered in ascending order. The formula for TE modes looks much the same, except that the tanh on the left-hand side is replaced by a coth, and that all dielectric constants are replaced by permeabilities.

Fig. 12 illustrates a number of the points which we have been making. It is the phase and amplitude plot of a dielectric slab placed on a large ground plane. The slab is indicated in black on the bottom of the picture, with the feed horn being just beyond the right-hand margin. The phase fronts are perpendicular to the slab near its surface, while the amplitude contours are essentially parallel and very densely packed due to the exponential decay (5 db per line). The slight

wiggle in the amplitude lines comes from a small reflected wave. The strong discontinuity on the left is due to the slab end. As a result of the very smooth transition from waveguide mode to trapped wave, the only disturbance in the vicinity of the feed is a group of amplitude islands on the extreme right which are some 35 db below the field intensity at the slab surface. The length of the antenna is such as to satisfy very nearly the Hansen - Woodyard condition for maximum gain: this can be seen by following the radiation from the region of the source, across the dielectric slab (where its phase is seen to interfere with the phase of the trapped wave), and into the main lobe region which begins on the extreme left and in which the original phase fronts align themselves quite well with the phase fronts arising at the terminal discontinuity.

To sum up, then, we might say that the process of radiation from trapped wave antennas seems well understood at the present time, that some of the basic information required for phase and amplitude control is now at hand, and that the introduction of phase and amplitude modulation along a trapped wave antenna should provide

us with beam shapes suitable for a great variety of applications.

REFERENCES

1. F.J. Zucker, "Theory and Applications of Surface Waves," Microwave Optics Symposium Issue, Supplemento No. 3, Nuovo Cimento 2 (1952). See also bibliography with this paper.
2. A.S. Dunbar, "On the Theory of Antenna Beam Shaping," J. Appl. Phys. 23, 847 (1952).
3. A.F. Kay and J. Kotik, paper to be published in the Proceedings of the McGill Symposium on Microwave Optics, to be issued by Air Force Cambridge Research Center in Summer, 1954.
4. R.S. Elliott, "On the Theory of Corrugated Plane Surfaces", TM 317, Contract AF 19(604)-262, Hughes Aircraft Company (1953).
5. Formerly at Hughes Aircraft Company, now with Microwave Radiation Company, Venice, California.
6. G.E. Mueller, "A Broadside Dielectric Antenna," Proc. I.R.E., 40, 71 (1952).
7. With the Compagnie de Telegraphie Sans Fils, Paris, France.

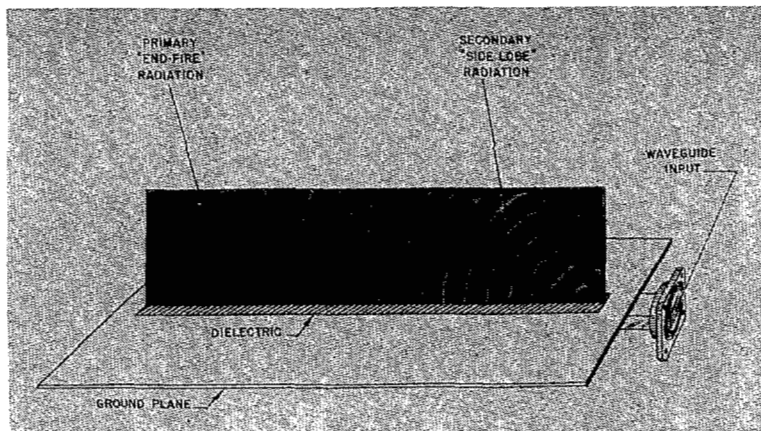
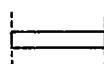
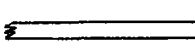


Fig. 1
Phase front contours of a metal-clad dielectric antenna.

The far field pattern of



is equivalent to



minus

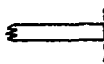
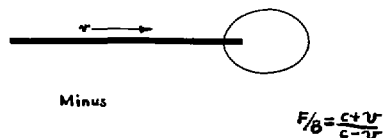


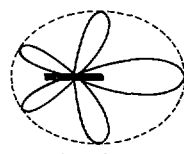
Fig. 2



Minus

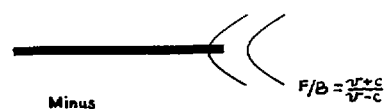
$$F/B = \frac{c+v}{c-v}$$

Equals



$$v < c$$

Fig. 3



Minus

$$F/B = \frac{v+c}{v-c}$$

Equals

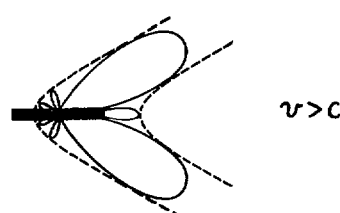


Fig. 4

Spectrum in region I: discrete; III: continuous;
II: discrete + continuous; IV: continuous.

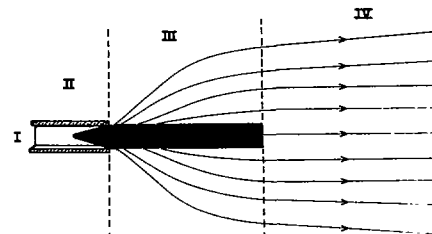


Fig. 5 - End-fire antennas.

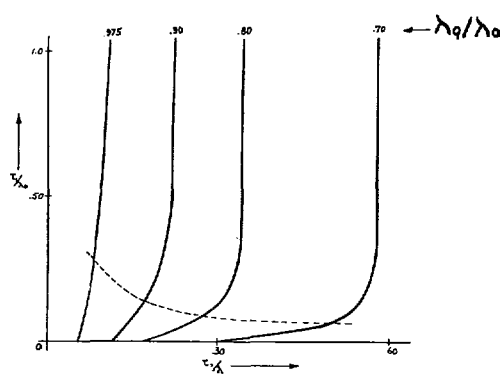


Fig. 6 - TM-mode.

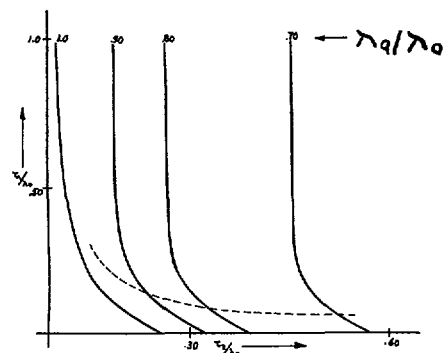


Fig. 7 - TE-mode.

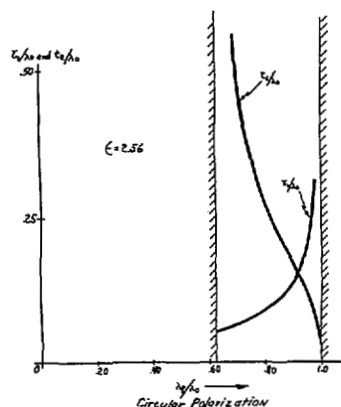


Fig. 8

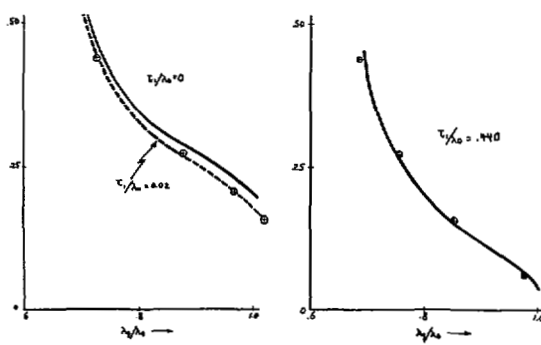


Fig. 9

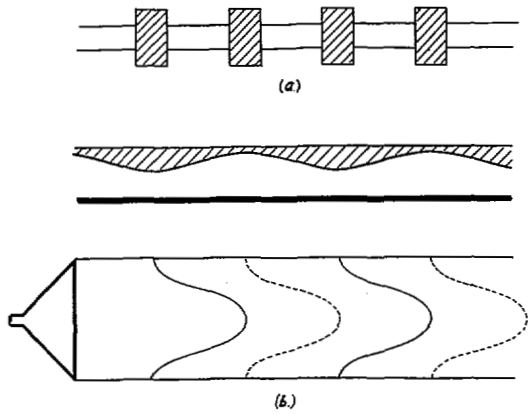


Fig. 10

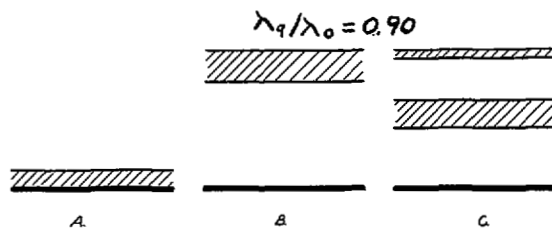


Fig. 11

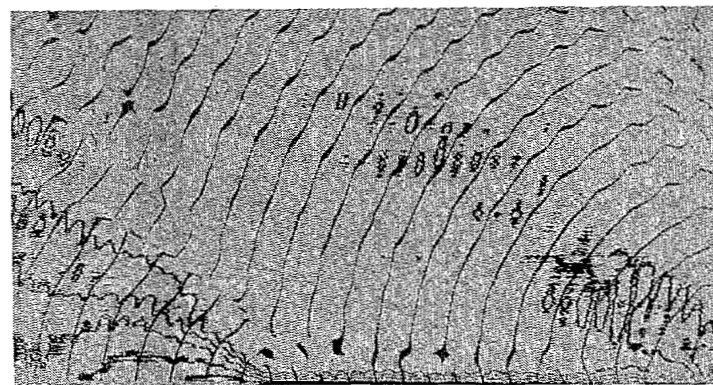


Fig. 12